Resonance Raman Spectroscopy of Squid and Bovine Visual Pigments: The Primary Photochemistry in Visual Transduction†

Mark Sulkes,‡ Aaron Lewis,* and Michael A. Marcus§

ABSTRACT: Resonance Raman spectra of squid rhodopsin have been obtained under a variety of temperature and illumination conditions. The data have been characterized in terms of spectral contributions from squid rhodopsin, isorhodopsin, bathorhodopsin, lumirhodopsin, mesorhodopsin, P-465, and acid metarhodopsin. The results are compared with the spectral features obtained from bovine rhodopsin, isorhodopsin, and bathorhodopsin. The data support a proposed structure for the chromophore in bathorhodopsin which is not all trans, 11-cis, or 9-cis. This structure can be generated from either rhodopsin or isorhodopsin by a similar motion (simultaneously rotating chromophore carbon atoms 10 and 11 out-of-plane). Furthermore, we detect the same distinct bathorhodopsin vibrational modes when rhodopsin is illuminated between 4 and 100 K. This demonstrates that under steady-state illumination the light-induced chromophore structural alterations occurring at 4 K are very similar to those occurring at higher temperatures. Finally, our data indicate that bathorhodopsin is generated not only by structural transitions in the chromophore but also alterations in the opsin conformation as has recently been proposed [Lewis, A. (1978) *Proc. Natl. Acad. Sci. U.S.A. 75*, 549].

Resonance Raman spectroscopy has emerged as an important method for studying biological molecules containing retinylidene chromophores (Lewis et al., 1973; Lewis & Spoonhower, 1974). By using radiation within the frequencies of the chromophore's electronic absorption, it is possible to obtain a resonance enhanced Raman spectrum of vibrational modes that are electronically coupled to the chromophore absorption (Lewis & Spoonhower, 1974; Tang & Albrecht, 1970). These studies have already supplied new information on the conformations of retinals and retinylidene chromophores (Rimai et al., 1971, 1973; Gill et al., 1971; Heyde et al., 1971; Cookingham et al., 1976, 1978; Cookingham & Lewis, 1978; Mathies et al., 1977; Callender et al., 1976), as well as confirming that the Schiff base retinylidene opsin link is protonated and can be deuterated in both rhodopsin (Lewis et al., 1973; Lewis & Spoonhower, 1974; Oseroff & Callender, 1974; Callender et al., 1976; Sulkes et al., 1976; Mathies et al., 1976) and bacteriorhodopsin (Lewis et al., 1974).

In this paper we have extended these studies to include squid visual pigments in order to understand in greater detail the differences and similarities in vertebrate and invertebrate photoreception. To interpret our results, we have characterized the resonance Raman spectra of squid rhodopsin, isorhodopsin, and bathorhodopsin using variable temperature and illumination conditions. The spectral features of these species are compared to high resolution (2 cm^{-1}) spectra of bovine photostationary mixtures obtained at similar temperature and illumination conditions. This comparison has resulted in a better understanding of both the bovine and squid spectra. Furthermore, our experimental results have also provided us with a detailed understanding of the structural transitions that are required to generate bathorhodopsin.

Squid and Bovine Intermediate Sequences. Figure 1 shows the intermediate sequence for the bovine (1A) and squid (1B) cases. Thermal steps are denoted by solid arrows and light-induced steps by dashed arrows. The "main line" of each sequence proceeds vertically downward. Light-induced back reactions to isorhodopsin or rhodopsin can take place from bathorhodopsin through metarhodopsin. In each case isorhodopsin is shown in a position analogous to rhodopsin at the beginning of the sequence. It is this identity of the bovine and squid intermediate sequences in the "photon initiation" portion that suggests strongly that the same photochemical principles are involved in each sequence.

Some time ago isorhodopsin was shown to occupy a position analogous to rhodopsin among the intermediates in low temperature work (Yoshizawa & Wald, 1963). But the role of isorhodopsin under physiological conditions, if any, remained open to question. Recently, however, Goldschmidt et al. (1976) have shown that bovine bathorhodopsin can be driven by light to isorhodopsin under physiological conditions as well. It was also recently demonstrated in skate retinas (Pepperberg et al., 1976) that isorhodopsin, like rhodopsin, produces light-initiated electrophysiological responses. Thus, isorhodopsin can generate the same bathorhodopsin intermediate as rhodopsin and can initiate visual excitation.

Differences in the retinylidene-opsin interactions of squid and bovine pigments show up increasingly as the thermal sequence proceeds. There is an additional intermediate, mesorhodopsin (Tokunaga et al., 1975; Azuma et al., 1975; Ebina et al., 1975), in the main line of the squid sequence, as well as a photon initiated side path entity, P-465 (Suzuki et al., 1976). The retinylidene-opsin interactions are evidently somewhat stronger in the later intermediates for bovine pigments. The bovine intermediates through meta II show chromophore CD effects, while squid metarhodopsin does not (and meso shows only a small chromophore CD effect). Also, successive intermediates in the squid sequence show markedly decreasing propensities to be light-converted to the 9-cis pigment isorhodopsin (Suzuki et al., 1976). The situation is not nearly as marked in the bovine case.

By acid metarhodopsin in squid the ratio of oscillator strengths f(meta)/(rhod) is $\approx$1.5, whereas f(meta I)/f(rhod) $\approx$ 1.2 in bovine (Burke et al., 1973). Since polyene conjugation,

† From the School of Applied and Engineering Physics, Cornell University, Ithaca, New York 14853. *Received February 22, 1978; revised manuscript received July 7, 1978.* This work was supported by a grant from the National Institutes of Health No. EY01377. In its initial phases this work was also supported by the Petroleum Research Fund, administered by the American Chemical Society, the Research Corporation, and the Sloan Foundation.

‡ Present address: Department of Chemistry, University of Chicago, Chicago, Ill.

§ Present address: Kodak Research Laboratories, Kodak Park B-81, Rochester, New York 14650.

0006-2960/78/0417-4712$01.00/0

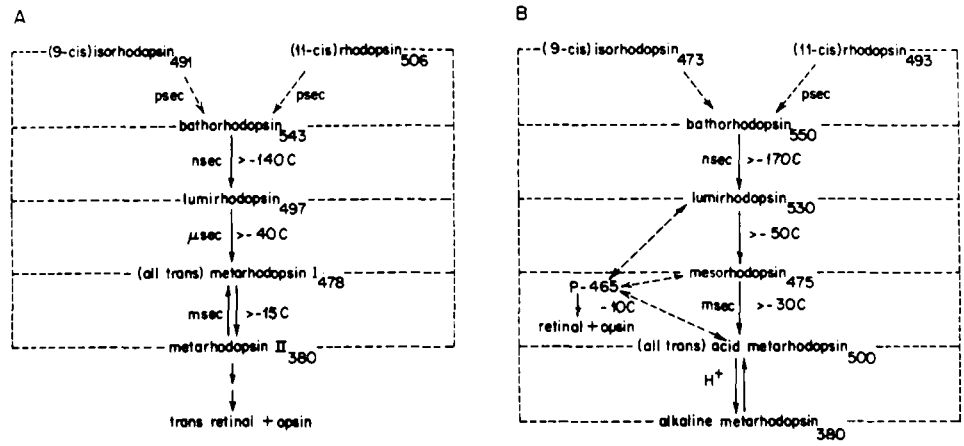

FIGURE 1: Intermediate sequences for (A) bovine and (B) squid photopigments. Dashed lines denote photon-induced transitions and solid lines thermal transitions.

and therefore f, should be maximum for an untwisted conformation, the suggestion here is that relaxation to an untwisted trans form has proceeded further in squid. These facts suggest that the Raman spectral features of intermediates late in the squid thermal sequence should be reproduced well by retinylidene model compounds, and we have already found this to be the case with acid metarhodopsin (Sulkes et al., 1976). It would then appear that modelling attempts might be less successful on the early "unrelaxed" thermal intermediates. This is the case for both bovine bathorhodopsin and squid bathorhodopsin, as we shall report and discuss and this may also be the case for squid lumirhodopsin.

Experimental Approaches. As we discussed elsewhere (Sulkes et al., 1976), the fact that squid metarhodopsin does not degrade to retinal plus opsin makes it an easy intermediate to study via Raman spectroscopy. This fact, together with the sensitivity of squid rhodopsin to denaturation, has prevented pigment reconstitution studies as have been done for bovine (Kropf et al., 1973; Honig & Ebrey, 1974) and bacterial (Marcus et al., 1977; Tokunaga et al., 1977) rhodopsin. As far as low temperature investigations of the early intermediates are concerned, these can proceed as in the bovine and bacterial cases (Oseroff & Callender, 1974; Lewis et al., 1974). The photostationary state concentrations of various intermediates present at low temperature will depend on the frequencies of illumination, relative photon fluxes, the pigment absorption cross sections at these frequencies, and their quantum efficiencies of conversion to other pigment forms. As in the bovine and bacterial cases, dual laser beam techniques are useful. One higher power "pump" beam is used to drive the photochemistry toward particular intermediates, while a second weaker beam is used to measure the Raman spectrum. Correlating peak size changes with the presence or absence of the pump beam is useful for assigning peaks to one intermediate or another (Oseroff & Callender, 1974).

Materials and Methods

Sample Preparation. All invertebrate experiments were on squid retinular suspensions in water. The eyes of dark-adapted squid (*Loligo pealii*) were removed under red light and stored on dry ice. The subsequent purification procedure of the retinular material was similar to those procedures carried out by other workers, such as Hubbard & St. George (1958). The impure suspension, in 0.1 M pH 6.5 phosphate buffer, which was obtained as in the Hubbard & St. George procedure, was layered on a 40% (by weight) sucrose solution (in 0.1 M phosphate buffer, pH 6.5) and centrifuged at 17 000 rpm for 20 min in a Sorval RC2B centrifuge with an SS34 head. The outer segments floated to the sucrose–buffer interface, while the impurities sedimented at the bottom of the tube. The outer segments were then drawn off and washed once in the buffer; then the flotation was repeated. Flotations were continued until no impurities were seen to sediment after centrifugation. The material was subsequently washed in the buffer, followed by three washings in doubly distilled water. All experimental manipulations were carried out under red light.

Suspensions in D_2O were also made. The material was pelleted and resuspended in D_2O. The D_2O was buffered to an effective pH of 6.5 in 0.1 M phosphate. The material was repelleted and resuspended in D_2O and then stored on ice in the dark. Preparations were allowed to equilibrate for at least 12 h before use.

To assay the material, absorption measurements were carried out on detergent-solubilized samples. For these experiments, a digitonin extraction was performed on several fractions of retinular material, each of several milliliters. The squid rhodopsin was solubilized in 2% digitonin in pH 6.5, 0.1 M phosphate for 3 h. The solution was centrifuged for 15 min at 15 000 rpm and the supernatant concentrated with a collodion bag concentration apparatus until the OD_{max} was ≈ 2 for a 1-cm optical path. The values obtained for the ratio of OD_{min} (λ = 403 nm) to OD_{max} (λ = 493 nm) generally ranged from 0.25 to 0.40. The addition of NH_2OH, which reduces the Schiff base of the chromophore in retinochrome but not rhodopsin (Sperling & Hubbard, 1975), causes a slight decrease in this ratio (of no more than ~1%), suggesting that only trace amounts of retinochrome could be present in the suspensions. A comparison of the Raman spectra of ROS suspensions with those of retinochrome (unpublished data) did not show any spectral features attributable to retinochrome. When the detergent solubilized material was run through a DEAE-cellulose column, there was not a marked improvement in the OD_{min}/OD_{max} ratio, suggesting that there is no significant problem with other impurities. Detergent extraction was not used to prepare samples for resonance Raman spectroscopy because Raman spectra could be obtained with retinular suspensions.

For the experiments on vertebrate rhodopsin, dark-adapted bovine retinas were purchased from George Hormel Co., Austin, Minn., and stored in liquid nitrogen until used. Bovine ROS were isolated as described by Applebury et al. (1974). Bovine ROS were solubilized in 2% Ammonyx-LO and purified on a hydroxylapatite column as described previously (Applebury et al., 1974). For the purified rhodopsin utilized in these experiments, the absorbance ratios were OD_{400}/OD_{500} = 0.20 and OD_{280}/OD_{500} = 2.0.

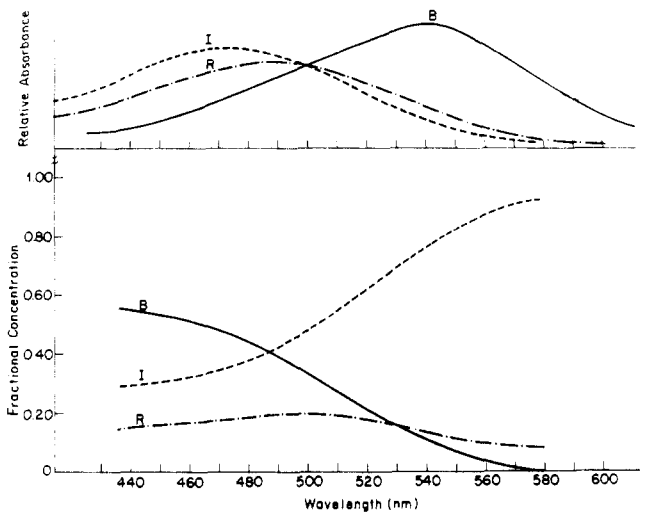

FIGURE 2: Calculated fractional photostationary concentrations vs. illumination frequency (one beam) for squid rhodopsin, isorhodopsin, and bathorhodopsin for temperatures below the transition to lumirhodopsin. In the upper part of the figure is shown the relative absorbances of these intermediates. The amount of resonance enhancement attained for each species increases as the Raman probe frequency enters its absorbance band.

Raman Spectroscopy. Spectra were obtained on two home-built systems, incorporating Spex 1401 and J-Y Ramanor HG-2 monochromators, each equipped with an RCA C31034 photomultiplier tube. Data points were acquired digitally in a stepped mode (Perreault et al., 1976) with 1 or 2 cm^{-1} steps. Laser power was continuously monitored with a photocell measuring a fraction of the beam reflected off a glass slide; counting time per channel (typically 20 s) was normalized for changes in laser power. Paper tape outputs were subsequently smoothed and plotted using a Modcomp 2 minicomputer and a Houston plotter. The laser sources used were a Coherent Radiation Model 53B krypton laser, a Model 52 argon laser, and a Model 490 dye laser using Rhodamine 6G dye pumped with a Coherent Radiation CR-12 argon laser. Extraneous fluorescence from the dye laser was eliminated by sending the beam through a home-built tunable optical filter (Collins et al., 1977); the ion laser beams were sent through interference filters. All experiments except the variable temperature studies used a 90° scattering geometry with a focused beam. For the variable temperature experiments a 180° scattering geometry was employed.

Dual beam experiments were performed by combining two laser beams with a 45° oriented beam splitter: this made the two beams coaxial. The coaxiality was checked at various points along the optical path, and the dual beam was passed through a circular aperture of ~1 mm diameter. This ensured that the illumination spot from each beam would be of the same size on the sample.

Sample volumes were relatively small. For the 273 K spectra, the suspension was placed in 2-mm i.d. Pyrex tubes, which were held in a copper block cooled to 273 K. In the liquid nitrogen runs, a single drop of the suspension was placed on the polished end of a 3-mm Pyrex rod that was immersed directly into the liquid nitrogen. The runs at variable low temperatures were undertaken in a Lake Shore Cryotronics "Spectrim" model closed cycle refrigeration cold head. The unit was capable of temperature regulation to within 1 K. Samples were placed in a 1-mm path length 3-mm thick quartz cuvette placed in a copper holder attached to the cold head.

The temperature in the sample as a function of temperature of the cold finger was measured using Stokes/anti-Stokes peak ratios of the 219 cm^{-1} band of CCl_4. The ratio is given by (Placzek, 1934)

$$\frac{I_S}{I_{AS}} = \left(\frac{\nu - \nu_R}{\nu + \nu_R}\right)^4 \exp\left(-\frac{r\nu_R}{kT}\right)$$

where ν_R is the reference peak vibrational frequency and ν the incident frequency. With the 219-cm^{-1} band it was possible, using I_S/I_{AS}, to make accurate temperature determinations in the range ~100–240 K. Temperature disparities between T(sample) and T(cold head) were, within experimental error, negligible in this range. Of course, it is possible in a resonance Raman situation (where an equation more complicated than the above one applies) that there may be slight temperature disparities, since the illuminated sample area is absorbing light. However, our variable temperature measurements were made at temperatures well within the thermal stability ranges of the intermediates under investigation.

Though a photostationary state is attained eventually at low temperatures, at some illumination frequencies small extinctions for an intermediate and/or relatively small quantum efficiencies for photochemistry can delay attainment of the steady state. Small changes in spectral features were in some cases observed to take place for several hours. Under each set of experimental circumstances spectra were run until reproducible results were obtained. In the low temperature spectra this sometimes necessitated a pre-spectrum illumination time of an hour or more. Multiple runs were always performed to verify that a photostationary state was reached.

The signal-to-noise ratio at 273 K was such that the large C=C stretch peak was generally two to three times the number of counts of the baseline. At 77 K this factor was generally around 4/3. The reduction of the signal-to-noise ratio at low temperatures primarily arose from increased fluorescence from the frozen samples. This fluorescent background rose as detection went further into the red. This fact made it difficult, unfortunately, to pump with a beam to the blue of the probe beam in order to produce a spectrum with predominantly bathorhodopsin bands. The resulting rising baselines were normalized to flatness on the computer by fitting analytical functions to them, then making the appropriate subtraction from the spectrum. In some of the low temperature and the deuterated spectra, multiple runs, each with identical spectral features, were pooled to produce a better signal-to-noise ratio. All wave number values as quoted are as in air.

Photostationary State Compositions. To establish quantitatively the relative concentrations of intermediates under each set of illumination conditions, calculations were carried out. Their accuracy depends on ratios of quantum efficiencies for intermediate conversions (γ) and extinctions of the intermediates (ϵ) at the illumination frequency (or frequencies, for two beam experiments), with relative photon fluxes also entering in the two beam case (see Appendix I). The calculated results for low temperatures (rhodopsin, isorhodopsin, and bathorhodopsin present) appear in Figure 2 along with relative intermediate absorbances. The practical experience for rhodopsins is that resonance enhancement is attained only if the incident frequency is within the absorbance band.

For the variable temperature results, as one blocks the thermal sequence further and further down the line, it is not necessarily true that only the latest intermediate will predominate in the spectrum. Each intermediate has light-driven back reactions to rhodopsin and isorhodopsin. In turn, these species can be photolyzed and "fall through" to the thermally blocked point. As a result, the photostationary state can contain some of the intermediates before the blocked point. However,

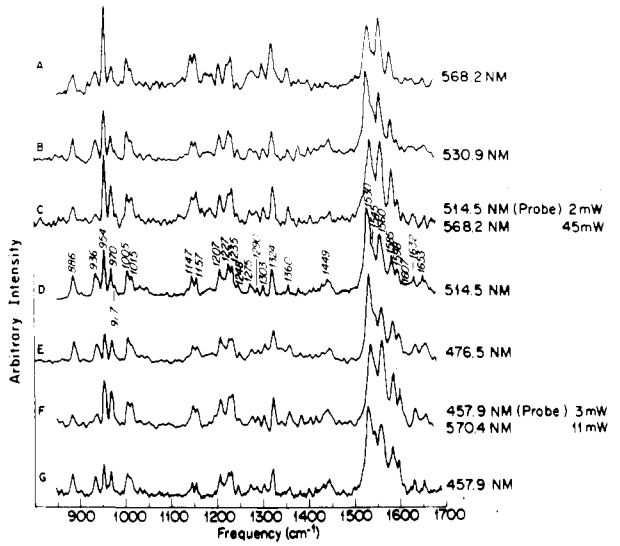

FIGURE 3: Spectra of squid photopigments at 77 K under a variety of illumination conditions, as indicated for each spectrum. The spectral slits were ~3 cm^{-1} in each case.

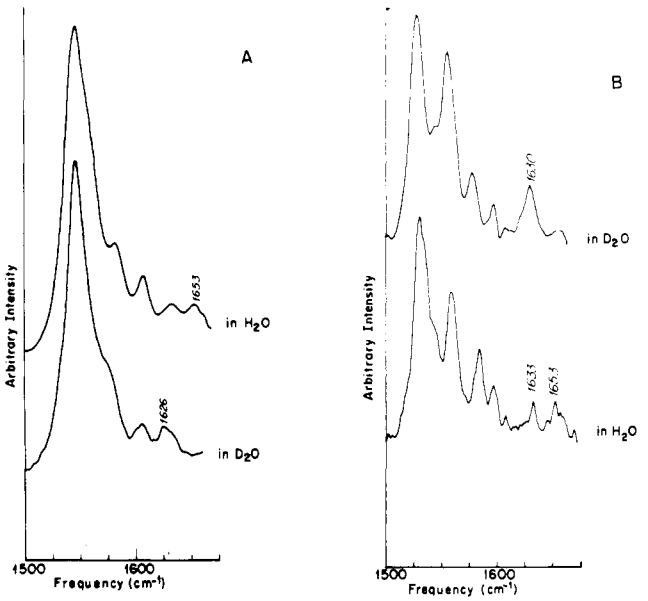

FIGURE 4: Raman spectra of deuterated and undeuterated squid pigment suspensions at (A) 273 K and (B) 77 K (~3 cm^{-1} slits) excited with 457.9-nm laser illumination.

only the immediately preceding thermally unstable intermediate should be present in significant amounts. The result is that the Raman spectra can become increasingly complicated until near-physiological temperatures are reached, where there is again a relatively simple photostationary state (i.e., the concentrations of the thermally unstable intermediates are negligible). At intermediate temperatures, the possibility of a large number of entities in the photostationary state produces much poorer spectra.

Protonated Schiff Base Preparations. 11-Cis and 9-cis protonated *N*-retinylidene-*n*-butylammonium hydrochloride ($N^+RB\ Cl^-$) solutions were prepared from the retinals. 11-*cis*-Retinal was a generous gift from Hoffmann-La Roche; 9-*cis*-retinal was purchased from Eastman Organic. The unprotonated butylamine samples were prepared as previously reported (Sulkes et al., 1976). The protonated Schiff bases were formed by bubbling HCl gas through an ethanolic solution of the unprotonated Schiff base. Resonance Raman spectra were obtained by flowing the solutions, which were kept in a cooled reservoir at −22 °C. The experimental setup has already been described (Cookingham et al., 1978). The exciting line used was 476.2 nm of a krypton ion laser.

Results

The data collected on squid rhodopsin are presented in Figures 3 to 6. The effect of illumination frequency on the character of the 77 K squid spectral features is displayed in Figure 3. Spectra of deuterated membrane fragment suspensions at 273 K and 77 K are shown in Figures 4A and 4B. The effects on the resonance Raman spectrum of varying the temperature between 50 K and 288 K are shown in Figure 5. Finally, in Figure 6 the 288 K and 50 K squid spectra are compared with all trans, 9-cis, and 11-cis protonated Schiff base spectra.

Discussion

Resonance Raman spectra of squid rhodopsin at 77 K are presented in Figure 3.[1] Spectra are shown at a variety of excitation frequencies because the most complete deconvolution of spectral features as to contributing intermediates can be seen in this way. Direct comparison, however, should be confined to spectra obtained with the same probe frequency (i.e., the same resonance enhancement factor). The introduction of a pump beam alters the relative concentrations of intermediates in the photostationary state. In the 457.9- and 514.5-nm spectra (Figures 3F and G and 3C and D, respectively), introduction of a yellow pump beam increases the concentrations of rhodopsin and isorhodopsin at the expense of bathorhodopsin (see Figure 2). At these frequencies one can see that the 886- and 936-cm^{-1} bands, for example, decrease relative to the 954- and 970-cm^{-1} bands when the pump beam is present. Hence the preliminary conclusion is that the 886- and 936-cm^{-1} peaks arise from bathorhodopsin. More detailed analysis of this kind, along with some supplemental criteria, allowed for intermediate assignments to be made for many bands in the spectra. These are indicated in Table I, along with the criteria used to arrive at the assignments.

A Comparison of Squid and Bovine Low Temperature Results. Although the spectra shown in Figure 3 bear some resemblance to the 80 K bovine resonance Raman spectra of Oseroff & Callender (1974), there are several differences. A low frequency mode appears in our squid spectra at 886 cm^{-1}, attributable to bathorhodopsin, unlike the bovine spectra, which have two bands, at 850 and 875 cm^{-1}, that are attributable to the batho intermediate. In addition, the region between 1500 and 1600 cm^{-1} shows strong multiple C=C stretching components for certain species. This has not been observed in either bovine or bacterial rhodopsin, and apparently is the first such observation in a rhodopsin. There are also other differences in this region that will be noted in the discussion.

Additional variations are also observed between 77 K spectra of squid rhodopsin (see Figure 3D) and the previously reported (Oseroff & Callender, 1974) bovine results. In order to resolve these differences we have repeated the Oseroff & Callender study at 2-cm^{-1} spectral resolution using 514.5-nm excitation (see Figure 7).[2] It is clear that our spectra at 2-cm^{-1} resolution

[1] Use of Figure 2 can help to rationalize some of the results of Figure 3. For instance, the 568.2-nm spectrum, though 90% isorhodopsin, has significant bathorhodopsin spectral components. The competition between single beam resonance enhancement and concentration effects is somewhat different here than in the bovine case, where 568.2-nm illumination produces a nearly pure isorhodopsin spectrum.

[2] The spectral features observed at ~4 K are identical with those at 95 K shown in Figure 7B. In addition, our data gave no indication of alterations in the squid photostationary state spectral features as the temperature was lowered from 100 to 25 K.

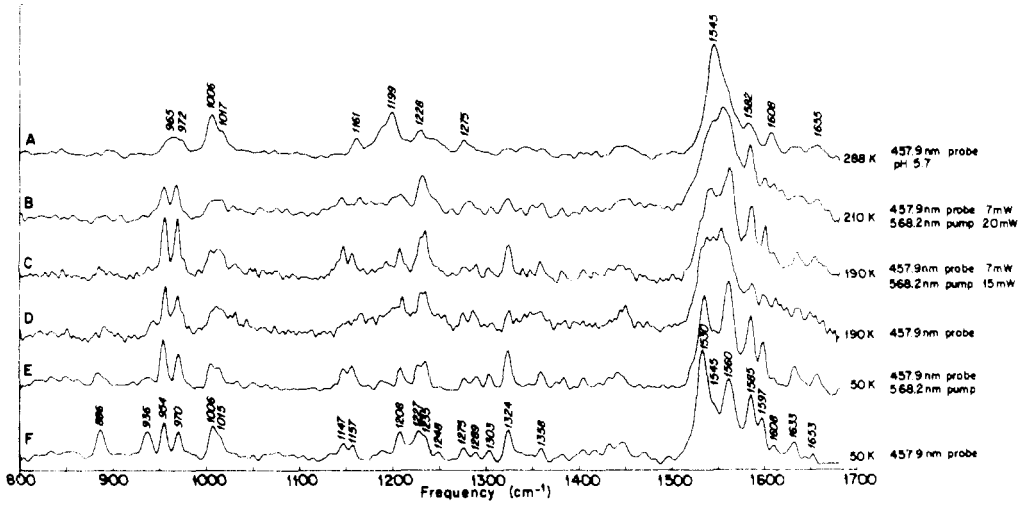

FIGURE 5: Squid photopigment spectra at a variety of temperature and illumination conditions, as indicated for each spectrum. Spectra E and F were obtained with 2-cm^{-1} steps and counting times of ~100 s/channel. The spectral slits were 3–4 cm^{-1} in all cases except E and F, where they were 5 cm^{-1}.

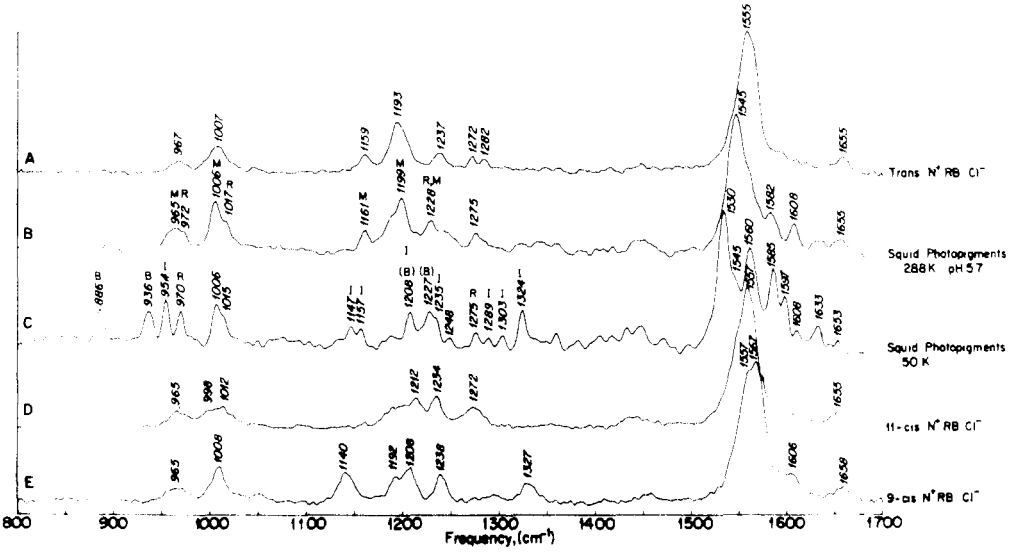

FIGURE 6: Comparison of 288 K and 50 K photopigment spectral features with those of all-trans, 9-cis, and 11-cis protonated Schiff base model compounds. The spectra shown are (A) *all-trans-N*-retinylidene-*n*-butylammonium hydrochloride ($N^+RB\ Cl^-$), 476.2-nm illumination; (B) a squid photopigment suspension at 288 K, 457.9-nm illumination; (C) a squid photopigment suspension at 50 K, 457.9-nm illumination; (D) 11-*cis*-$N^+RB\ Cl^-$, 476.2-nm illumination; and (E) 9-*cis*-$N^+RB\ Cl^-$, 476.2-nm illumination. The spectral slits in each case were 3–4 cm^{-1} except for C, where they were 5 cm^{-1}. The all-trans, 9-cis, and 11-cis spectra were obtained in ethanol solutions. In the squid photopigment spectra B and C, band assignments for acid metarhodopsin (M), rhodopsin (R), isorhodopsin (I), and bathorhodopsin (B) are indicated for the major intermediate contributing. Tentative assignments are put in parentheses. In some cases, contributions from other species are possible but have not been unambiguously confirmed. For example, rhodopsin certainly contributes to the bands in the region between 1200 and 1250 cm^{-1} as indicated by the bovine spectra (Figure 7B). In addition, unlabeled bands cannot be unambiguously assigned at this time. The reader is referred to the text for a discussion of some of these bands.

show details that are "blurred" in the earlier 8-cm^{-1} study of bovine rhodopsin at 80 K. An important example of this effect can be seen by considering the squid photopigment C–H bend bands at 954, 970, and 977 cm^{-1} (see Figure 3D). The spectra shown in Figure 3 indicate that these C–H bend vibrational modes can be ascribed to isorhodopsin, rhodopsin, and bathorhodopsin, respectively. Previously, the study of Oseroff & Callender (1974) had ascribed a single 967-cm^{-1} band to the C–H bend. Our bovine spectrum shown in Figure 7B is compared with a 77 K squid spectrum (Figure 7A) also taken with 514.5-nm illumination. It is clear that in this bovine spectrum there are three separate bands in the region between 950 and 980 cm^{-1} where C–H bends are expected, one band for each species present. There appears to be a direct correspondence between these three bands and the vibrational frequencies observed in the squid spectrum (see Figure 7A). Based on the spectra in Figure 3, the 970-cm^{-1} band can be assigned to squid rhodopsin and is similar to the 970-cm^{-1} band observed in our 77 K bovine spectrum (Figure 7B) and in spectra of bovine rhodopsin reported by other workers (Mathies et al., 1976; Callender et al., 1976). Similarly, a band at 954 cm^{-1} in our 77 K squid spectra can be associated with isorhodopsin. There is a similar band at 958 cm^{-1} in our bovine spectrum, which is also in agreement with the frequency of the C–H bend for bovine isorhodopsin obtained by flow measurements (Mathies et al., 1976). Therefore it appears very likely that the 977-cm^{-1} vibration in squid batho and the 980-cm^{-1} band in bovine are the C–H bend bands of these species.

A further indication of the effect of resolution is the apparent lack of a strong correlation between our data on squid rhodopsin and the earlier bovine study in the region between 1000 and 1500 cm^{-1}. However, our resolution of bands at 1000,

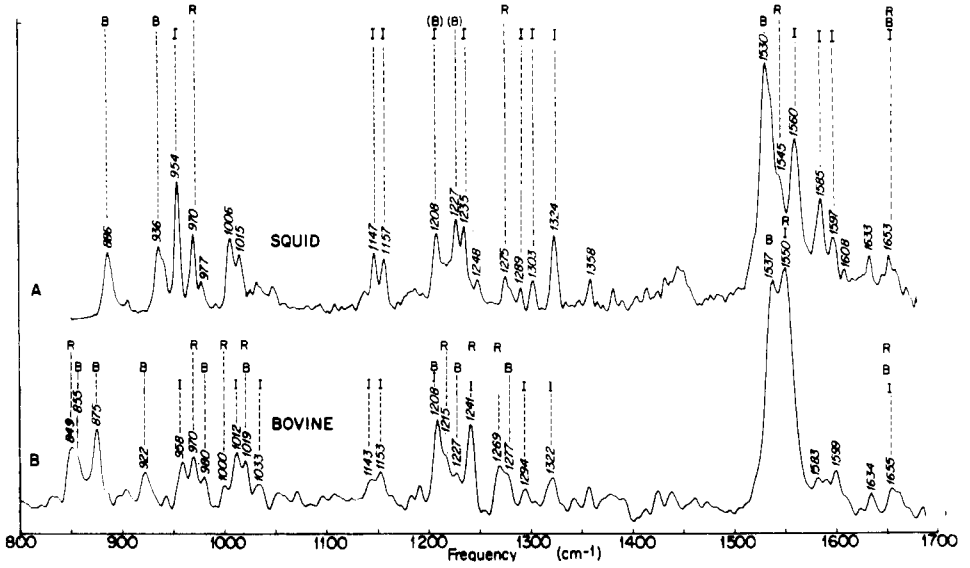

FIGURE 7: Low-temperature bovine and squid spectra taken with 514.5-nm illumination. The squid spectrum (A) was taken at 77 K with 3-cm^{-1} spectral slits. The bovine spectrum (B) is at 95 K with 2-cm^{-1} spectral slits. No bands were observed from 800 to 500 cm^{-1} in the squid case (see Figure 3). Proposed band assignments are indicated and the labeling is the same as in Figure 6. The reader is also referred to the cautions on these band assignments indicated in the Figure 6 caption.

TABLE I: Assignment of Major Bands in the Low Temperature Squid Spectra to Rhodopsin (R), Isorhodopsin (I), and Bathorhodopsin (B).[a]

band (cm^{-1})	assignment
886	B
936	B
954	I
970	R
977	B (?)
1006	B (?)
1015	I (?)
1017	R
1147	I
1157	I
1208	I, B (?)
1227	B (?)
1235	I
1248	B (?)
1275	R
1289	I
1303	I
1324	I
1358	I (?)
1530	B
1545	R
1560	I
1585	I
1598	I
1608	R
1632	I (?)
1653	R, I, B

[a] The assignments were arrived at by means of comparison of dual and single beam spectra with the same probe frequency and by comparison of spectra taken under the same illumination conditions but at different temperatures, where there are differences in the photostationary state. Further descriptions of most assignments are in the text. The assignments in the region from 1000 to 1500 cm^{-1} are for the major intermediate contributing to the band in the photostationary mixtures we were able to obtain; contributions from other intermediates are possible in some cases. The reader is also referred to the Figure 6 caption for further cautions on these band assignments.

1012, 1019, 1143, and 1227 cm^{-1} in the bovine spectrum (Figure 7B) reveals a detailed correlation between the squid and bovine low temperature resonance Raman spectra in this region.

Deuteration Results at 273 K and 77 K. A comparison of resonance Raman spectra of retinular membrane fragment suspensions in D_2O and H_2O is shown in Figure 4. Figures 4A and 4B show the results at 273 K/pH(effective) 6.5 and 77 K/pH (effective) 6.5, respectively. At 273 K rhodopsin and acid metarhodopsin predominate and at liquid nitrogen temperature rhodopsin, isorhodopsin, and bathorhodopsin are present. Rhodopsin is common to both situations. Assuming a pure $-C{=}N^{+}H-$ stretch, the replacement of the proton mass by a deuteron mass should cause a frequency downshift of the band from 1653 to ~1630 cm^{-1}, and this result was observed at both temperatures. Since the 1653-cm^{-1} bands at 273 K and 77 K have disappeared as a whole, this suggests that evidently rhodopsin, isorhodopsin, bathorhodopsin, and acid metarhodopsin all exist as protonated Schiff bases.

Even though the deuteration results suggest that all the species present in our spectra at 273 K and 77 K are fully protonated, there is a band that appears in both the 273 K and 77 K spectra at ~1630 cm^{-1}. There is no evidence in our spectra that this band is associated with a partially protonated Schiff base since it is not detectably affected by deuteration. Furthermore, there is no evidence in our 77 K spectra of a 1620-cm^{-1} band which is the vibrational frequency of a completely deprotonated Schiff base. Therefore, the only consistent explanation for our results is that all four species, rhodopsin, isorhodopsin, bathorhodopsin, and acid metarhodopsin, are fully protonated Schiff bases. The above, of course, does not rule out the possibility that the Schiff base proton temporarily changes its position in the excited state between rhodopsin/isorhodopsin and bathorhodopsin. However, it should be noted that it is very unlikely that such an effect alone could account for the large deuterium isotope effect observed by Peters et al., (1977) on the rate of formation of bovine bathorhodopsin.

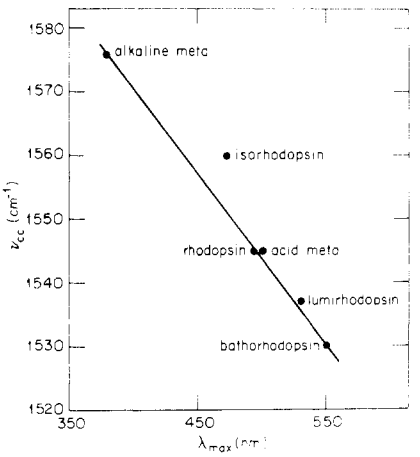

FIGURE 8: Correlation plot of $\nu_{C=C}$ vs. λ_{max}(absorption) for observed squid photopigment intermediates.

C=C Stretching Frequencies from 1500 to 1600 cm^{-1}. There is a rather interesting difference between the two isorhodopsins (bovine and squid) in the C=C stretching region. The C=C stretch of bovine isorhodopsin has one large component at 1550 cm^{-1}. By contrast, in squid isorhodopsin strong components appear at 1560, 1584, and 1598 cm^{-1}.[3] This is especially interesting in view of the fact that there are detailed similarities in the modes between 1000 and 1500 cm^{-1} in squid and bovine isorhodopsin (Figures 7A and 7B). The similarity of this conformationally sensitive region in bovine and squid suggests that factors other than conformation are causing these multiple C=C stretches. Warshel & Karplus (1974) have shown for the 9-cis isomer that multiple C=C stretches can develop as a result of conformational strain in the chromophore. However, their calculations also predicted that other regions of the spectra are drastically altered. Thus, this suggests that our observation of multiple C=C stretches of significant intensity in squid isorhodopsin could result from different opsin charge perturbations of the 9-cis chromophore in bovine and squid isorhodopsin.

Our results on isorhodopsin do not support the suggestion of Aton et al. (1977) that a general correlation exists between the C=C stretching frequency and absorption maxima of retinylidene chromophores in all rhodopsin and bacteriorhodopsin protein environments. As can be seen in Figure 8, plots of the C=C stretching frequencies for six intermediates in the squid sequence vs. λ_{max} in nm show that even for one species a single straight line cannot be drawn through all points. However, some of the points in Figure 8 do fall on a straight line. This may be fortuitous or may arise from the fact that a large part of the total red shift in going from an unprotonated Schiff base (e.g., alkaline metarhodopsin) to protonated Schiff base species arises from π delocalization. Even from this latter point of view there are several results that cannot be explained. For example, given the straight line drawn through some points in Figure 8 one would predict for bovine bathorhodopsin (λ_{max} = 543 nm) a C=C stretching frequency of ~1532 cm^{-1}. Instead, as is seen in Figure 7B, a frequency of 1537 cm^{-1} is actually observed. Furthermore, squid bathorhodopsin and bacteriorhodopsin (bR_{570}) both have C=C stretching frequencies at 1530 cm^{-1} but their absorption maxima are 550 and 570 nm, respectively. Thus, all these results support the conclusion that a general linear correlation as proposed by Aton et al. does not exist. This probably arises from several factors including conformational strain in the chromophore and/or significant opsin charge perturbations which can partially control the color of visual pigments as a result of chromophore excited state stabilization [as suggested by the experiments of Sulkes et al. (1976) and the calculations of Honig et al. (1976)]. It should be noted, however, that the above results do not rule out the possibility of a "C=C stretch vs. λ_{max}" linear correlation in such systems as free retinylidene chromophores in different solution environments or possibly even the photointermediates of bacteriorhodopsin in which severe conformational strain may not exist.

C-H Bend. This band has a significantly greater intensity in isorhodopsin and rhodopsin than in acid metarhodopsin. This increased relative intensity of the C-H bend can be seen by considering the variable temperature spectra in Figure 5, as described below or by comparing the data of Sulkes et al. (1976) on metarhodopsin with the results of Mathies et al. (1976) and Mathies et al. (1977) on rhodopsin and isorhodopsin. Spectra 5A and 5F have a component arising from the rhodopsin C-H bend at ~970 cm^{-1}. As is evident from Figure 5F, the intensity of the band is comparable to the shoulder at ~1015 cm^{-1}, which arises from a methyl stretch component that can be attributed to the small concentration of rhodopsin present. This is once again the case in Figure 5A, where acid metarhodopsin is the major spectral species with rhodopsin also contributing. By contrast, in spectrum 5A there is now also a 965-cm^{-1} component arising from the C-H bend in acid metarhodopsin that is clearly smaller then the 1006-cm^{-1} acid metarhodopsin methyl stretch band. On the other hand, the extent of π delocalization in acid metarhodopsin and rhodopsin is similar, as evidenced by their identical $\nu_{C=C}$ at 1545 cm^{-1}. Therefore, the intensity differences must arise from excited state interactions present in rhodopsin but absent in acid metarhodopsin and model compounds (see Figures 6A, 6D, and 6E). Similarly, isorhodopsin also has a relatively intense C-H bend component. Thus, the excited state interactions present in rhodopsin must also be affecting the intensity of this band in isorhodopsin. Furthermore, since the C-H bend arises predominantly from the H's on the isoprenoid chain which are close to the Schiff base (Marcus & Lewis, 1978a), the intensity increase observed in this vibrational band when 9-cis and 11-cis are complexed to opsin indicates that the excited state opsin-chromophore interactions giving rise to this intensity change probably occur in this region of the isoprenoid chain.

Thus, these C-H bend data suggest that, in addition to the ground/excited state interactions regulating color, there is an additional vertically excited state interaction in visual pigments along the isoprenoid chain near the Schiff base. It appears that this additional opsin-retinal interaction does not affect the color or the $\nu_{C=C}$ of these pigments, since acid metarhodopsin and rhodopsin have the same $\nu_{C=C}$ and nearly the same λ_{max} but drastically different C-H bend intensities. Similarly, bacteriorhodopsin, like acid metarhodopsin, has a relatively weak C-H bend, but its absorption is also significantly red shifted, as discussed above.

Analysis of the Variable Temperature Spectra. Several general comments can be made on the resonance Raman spectra of squid photostationary mixtures recorded as a function of temperature (see Figure 5). It can be seen that, as the temperature is raised from 50 K (Figures 5E and F) to 190 K (Figure 5D), the C=C stretch of bathorhodopsin at 1530 cm^{-1} decreases in intensity to a shoulder, the C=C stretching frequencies of isorhodopsin decrease significantly in intensity,

[3] Even though reference to our higher resolution bovine results (Figure 7B) shows that there are relatively weak bands at 1583, 1590, and 1600 cm^{-1} that can be ascribed to bovine isorhodopsin, the point remains that in bovine isorhodopsin there is only one strong C=C stretch component.

and three new peaks appear between the 1530-cm^{-1} bathorhodopsin shoulder and the 1560-cm^{-1} isorhodopsin shoulder. These three new peaks are at 1537, 1545, and 1552 cm^{-1}. The 1545-cm^{-1} peak is present at 210 and 288 K and thus is assigned to rhodopsin, which should be present in all these photostationary mixtures. On the other hand, the 1537-cm^{-1} band disappears at 210 K and the 1552-cm^{-1} band becomes a weak shoulder at 288 K. Based on these results, the 1537-cm^{-1} band is in all probability associated with lumirhodopsin and the 1552-cm^{-1} peak may be associated with contributions from both P-465 and mesorhodopsin. In view of these assignments, it is interesting to note that in the 190 K spectrum (Figure 5D) there is a significant decrease in the 886- and 936-cm^{-1} low-frequency modes and increased scattering at 905 cm^{-1}. In addition, significant scattering is detected in this spectrum at ~1165 cm^{-1} and a definite doublet is observed at 1275 and 1285 cm^{-1} (without the presence of a 568.2-nm pump beam which normally increases the intensity of the 1289-cm^{-1} band at low temperatures, as a result of isorhodopsin contributions, thus giving the appearance of a 1275 cm^{-1}/1289 cm^{-1} doublet). These data may indicate that lumirhodopsin, which is present at 190 K, has some features that are characteristic of all trans-protonated Schiff bases of retinal (scattering at ~1165 cm^{-1} and a 1275 cm^{-1}/1285 cm^{-1} doublet), although there are other aspects of this spectrum (Figure 5D), such as the scattering at 905 cm^{-1} and the lack of intense scattering between 1170 and 1200 cm^{-1}, which seem to indicate that the chromophore in lumirodopsin is not in an unperturbed all-trans conformation. One note of caution should be added to these assignments. It is obvious from Figure 5D that mesorhodopsin and/or P-465 may be contributing to this spectrum and this may complicate the assignments. However, single beam (457.9 nm) spectra at temperatures between 210 and 250 K (unpublished data), which appear to have significant mesorhodopsin and/or P-465 contributions, do exhibit intense scattering between 1170 and 1200 cm^{-1} which is not present in the 190 K spectrum (Figure 5D). This gives us additional confidence in the above suggestions on the lumirhodopsin chromophore conformation.

Assigning Bathorhodopsin Spectral Features. A. C=C Stretching Frequency: As has been discussed above, the C=C stretching frequency ($\nu_{C=C}$) is reduced when squid rhodopsin is photochemically converted to bathorhodopsin. This has been observed previously (Oseroff & Callender, 1974) in bovine rhodopsin. However, our squid results indicate that $\nu_{C=C}$ is reduced by 15 cm^{-1} rather than the 8 cm^{-1} decrease observed in bovine rhodopsin (see Figures 7A and 7B). This reduction in $\nu_{C=C}$ could be indicating that the bathorhodopsin chromophore structure is distorted around double bonds.

B. The C-CH_3 Stretch and Fingerprint Region: Assigning the Spectra. The region we will now consider extends from 1000 to 1500 cm^{-1} and provides detailed information on the conformation of the retinylidene chromophore (Heyde et al., 1971; Cookingham et al., 1976). Use of the dual beam technique allows a partial deduction of which bands bathorhodopsin does or does not contribute to in this region. In order to obtain such information reliably, spectra have to be recorded with low noise levels. Examples of such data are shown in Figures 5E and 5F. In going from spectrum 5F to 5E, the concentration of batho decreases significantly (from ~50% of the mixture to ~10%), and isorhodopsin is the principal component that gains from this decrease. This can be seen in the 900-cm^{-1} bend region of the spectrum by noting that the 936-cm^{-1} batho peak decreases significantly, while the ratio of the 954-cm^{-1} (isorhodopsin) peak to the 970-cm^{-1} (rhodopsin) peak increases.

This same effect (i.e., an increase in isorhodopsin) also is seen in the region between 1000 and 1500 cm^{-1}. Bands at 1015, 1147, 1157, 1235, and 1324 cm^{-1} increase relative to the other spectral features in this region in going from Figure 5F to 5E, indicating isorhodopsin contributions. These assignments are supported by the variable temperature results (e.g., Figure 5C), where isorhodopsin persists as a major component, and these data also indicate that isorhodopsin makes a significant contribution to the band at 1208 cm^{-1}.

Except for the 1147-cm^{-1} band, these spectral assignments for isorhodopsin are in good agreement with the low temperature (Oseroff & Callender, 1974) and room temperature flow spectra (Mathies et al., 1976) of bovine isorhodopsin in the fingerprint region. However, each of these bovine spectra shows a single isorhodopsin band at 1153 cm^{-1}, and it was on this basis that we concluded earlier (Sulkes et al., 1976) that the 1147-cm^{-1} band in a 77 K squid suspension must be due to bathorhodopsin, since a comparison with our 273 K spectra showed that rhodopsin did not contribute at 1147 cm^{-1}. At this point we note, however, that our higher resolution bovine spectra (see Figure 7B) show that the 1153-cm^{-1} component reported earlier by Oseroff & Callender is in actuality composed of two bands, one at 1143 cm^{-1} and one at 1153 cm^{-1}. Evidently, the earlier results on bovine isorhodopsin, obtained with 8-cm^{-1} resolution at 80 K and 6.6-cm^{-1} resolution at room temperature (with additional temperature broadening of bands), resolved these spectral features as a composite peak at 1153 cm^{-1}. In addition, our 2-cm^{-1} low temperature bovine spectra taken with 568.2-nm illumination (~98% isorhodopsin) also show an 1143/1153 cm^{-1} splitting. Thus, on the basis of our higher resolution bovine spectra and our variable temperature results, we reassign the 1147-cm^{-1} component as arising mainly from isorhodopsin.

Bands at 1289, 1303, and 1358 cm^{-1} are also probably due to isorhodopsin. These assignments are based on the increase in their intensities between Figures 5E and 5F and their persistence in Figures 5B through 5D. This is also supported by their virtual disappearance on going to the 288 K spectra (Figure 5A), which has little isorhodopsin contribution.

The above analysis of the dual beam and variable temperature data suggests that in squid photostationary state mixtures bathorhodopsin definitely contributes to the 886-, 936-, 1530-, and 1653-cm^{-1} bands. It also probably contributes to the 1208- and 1227-cm^{-1} fingerprint modes and there is also some evidence in the spectra to indicate that bathorhodopsin is responsible for the bands at 977, 1006, and possibly even 1248 cm^{-1}. The tentative nature of these assignments in squid arises mainly from the lack of pure isorhodopsin and rhodopsin data. The availability of such data at high resolution in bovine rhodopsin allows for definitive assignments of the photostationary state bovine spectra (Marcus & Lewis, 1978b) and these assignments are shown in Figure 7B. Thus, we can now compare the spectral features in rhodopsin and bathorhodopsin and this should help us characterize the structure of the chromophore in bathorhodopsin.

Comparing Rhodopsin and Bathorhodopsin Spectral Features. A vibrational mode that is characteristic of the 11-cis configuration is the splitting of the C-CH_3 stretch into two components (Cookingham & Lewis, 1978), at 1000 and 1019 cm^{-1} in bovine rhodopsin. This is clearly seen in our high resolution low temperature spectra (Figure 7B), with an additional band at 1012 cm^{-1} which arises from isorhodopsin. Bathorhodopsin appears to contribute only to the mode at 1019 cm^{-1} (unpublished dual beam spectra). In assigning the squid photostationary state mixtures, however, the lack of pure rhodopsin and isorhodopsin spectra makes it much more dif-

ficult to assign the modes observed in this region, although it does appear that rhodopsin and isorhodopsin contribute to the band at 1015 cm^{-1}, whereas bathorhodopsin contributes only to the band at 1006 cm^{-1}. This is based on the dual beam and variable temperature spectra. Thus, the data indicate that, although the rhodopsin chromophore has two C-CH_3 bands at 1000 and ~1019 cm^{-1} which are characteristic of the 11-cis configuration, bathorhodopsin appears to have only a single contribution at a frequency between 1000 and 1017 cm^{-1}.

The presence in bathorhodopsin of only one band in the 1000-cm^{-1} region is consistent with an all trans conformation for the chromophore, as seen in the modeling of acid metarhodopsin (compare Figure 6B with 6A). However, our modeling study of acid metarhodopsin also established (Sulkes et al., 1976) that all trans chromophores have significant scattering between 1190 and 1200 cm^{-1} and at ~1160 cm^{-1} and bathorhodopsin does not contribute significantly to either of these regions (see Figures 6C and 6B). Therefore there must be an alternative interpretation for the presence of a single C-CH_3 stretch.

In order to reconcile these seemingly contradictory pieces of data on bathorhodopsin and to explain the origin of the vibrations between 800 and 900 cm^{-1} (that are absent in 11-*cis*-, 9-*cis*-, or *all-trans*-N^+RB but present in bathorhodopsin), let us consider in more detail the origin of the C-CH_3 splitting in 11-cis conformations. It has been shown (Cookingham & Lewis, 1978; Cookingham et al., 1978) that 11-cis chromophores in both the 12-*s*-trans and 12-*s*-cis conformations exhibit a splitting in the C-CH_3 vibration. This appears to result from the structural constraints imposed on the 11-cis isomer in either of these two conformers. However, resonance Raman spectra of 11-*cis*-retinal in solution, recorded as a function of temperature (Cookingham & Lewis, 1978; Cookingham et al., 1978), indicate that the 11-cis-12-*s*-trans conformer has stronger scattering at 1275 cm^{-1}. This is supported by analogue data (Cookingham & Lewis, 1978; Cookingham et al., 1978) on 11-cis isomers that can achieve only the *s*-cis conformation. These isomers exhibit only weak scattering in this region. Thus, the presence of a strong 1275-cm^{-1} band in rhodopsin suggests that the chromophore is in a 12-*s*-trans conformation to begin with. This conclusion is supported by analogue pigment experiments (Ebrey et al., 1975; Chan et al., 1974) on bovine rhodopsin. However, there is no evidence to indicate that the chromophore is 11-cis 12-*s*-cis or 12-*s*-trans in batho, since the C-CH_3 splitting has coalesced into one peak. Similarly, just as the batho spectra do not contain characteristic 11-cis-12-*s*-cis/12-*s*-trans and all-trans bands, it also does not contain the 9-cis bands at 1147 and 1157 cm^{-1}.

A structure which is not 11-cis, 9-cis, or all-trans and has similar environments for the C-9 and C-13 methyl groups, which would suggest no C-CH_3 splitting, has been proposed by Lewis (1978). The serious out-of-plane distortion in this molecular structure is obtained by simultaneous rotation of chromophore carbon atoms 10 and 11 out-of-plane and could explain the origin of the intense low frequency vibrational modes in squid bathorhodopsin. It should be noted that such modes are not present in acid metarhodopsin or in spectra of 11-cis, 9-cis, or all-trans N^+RB model compounds (see Figures 6B, D, E, and A). In fact, normal coordinate calculations completed in our laboratory on such a distorted structure show drastically altered vibrational modes below 900 cm^{-1}.

Bovine bathorhodopsin exhibits an additional intense vibrational mode in this region and bovine rhodopsin also has a band in this region. This could arise from ring distortions in bovine bathorhodopsin which are not present in squid bathorhodopsin. Such ring distortions would affect the resonance Raman spectrum below 900 cm^{-1} with little or no effect above this frequency [(see Figure 4C of Warshel (1977)].

Finally, an important attribute of the structure proposed by Lewis (1978) is that it is common to both the 9-cis and 11-cis configurations and is produced by a similar torsional motion in each case. This is a characteristic which is essential in explaining the observation that either 11-cis (rhodopsin) or 9-cis (isorhodopsin) generates the same bathorhodopsin intermediate at low temperatures (Yoshizawa & Wald, 1964) and even in picoseconds at room temperature (Busch et al., 1972; Green et al., 1977).[4]

The Primary Mechanism of Excitation. All of the structural data discussed above indicates that the primary mechanism of excitation in visual transduction is not an 11-cis to all-trans isomerization. What appears to be fundamental from these data in both the bovine and squid systems is that there is a distorted 11-cis or 9-cis structure which bears little resemblance to changes that can be characterized as a cis–trans isomerization. However, this structure must allow for subsequent relaxation to an all-trans conformation, and in our proposed model for the batho chromophore such a process could occur via partial rotations around the C_9–C_{10} and C_{11}–C_{12} bonds.

Let us now consider what photon-induced events can give rise to such a distorted conformation. It is evident from our discussion of the color of visual pigments that one of the primary results of photon absorption is a significant electron redistribution in the chromophore. As has been pointed out (Lewis, 1978), this electron redistribution may bring about opsin structural alterations. In such a mechanism the chromophore could subsequently achieve distorted conformations which would stabilize the new protein structure induced by light. The presence of such light induced opsin structural alterations is supported when the deuterium isotope effect on the time evolution of bathorhodopsin, detected by Peters et al. (1977), is interpreted in light of the data presented on the -C=N^+H- stretch in this paper. Our results demonstrate that the -C=N^+H- stretch is unaltered in going from rhodopsin to bathorhodopsin. This indicates that the only exchangeable proton on the chromophore (the Schiff base proton) does not change its position as a result of the photochemistry. Therefore, the large deuterium isotope effect detected in the Peters et al. experiment results for the most part from proton movement within the protein matrix and not in the chromophore. Thus, all our results support the molecular mechanism of excitation proposed by Lewis (1978) in which both protein and chromophore structural alterations are essential for the production of bathorhodopsin.

Appendix 1: Photostationary Concentrations of Squid Rhodopsin, Isorhodopsin, and Bathorhodopsin at Low Temperature

The light-induced changes between rhodopsin, bathorhodopsin, and isorhodopsin can be schematized as follows, where

[4] It should be pointed out that the above deductions on the chromophore structure assume that a distorted conformation is the principal cause for the unique bathorhodopsin vibrational modes observed in the spectrum. Although this is the simplest explanation for the data, our recent results on bacteriorhodopsin (Marcus & Lewis, 1978a) indicate that future experiments should be aimed at investigating the role of the protein in producing some of these unique bathorhodopsin vibrational modes. In addition, further work is also required to determine whether model compound data on relaxed chromophores can be applied to bathorodopsin, which may have a distorted retinal conformation. However, it should be noted in this regard that the modes we focused on in this discussion (such as the C-9 and C-13 C-CH_3 stretch) would probably have a very similar admixture of vibrations in relaxed and distorted chromophores.

k's are rate constants:

$$R \underset{k_{br}}{\overset{k_{rb}}{\rightleftharpoons}} B \underset{k_{ib}}{\overset{k_{bi}}{\rightleftharpoons}} I \quad (1)$$

To obtain fractional compositions, steady-state conditions can be applied. The resulting equations are:

$$\% R = \frac{k_{br}/k_{rb}}{k_{br}/k_{rb} + k_{bi}/k_{ib} + 1} \quad (2a)$$

$$\% I = \frac{k_{bi}/k_{ib}}{k_{br}/k_{rb} + k_{bi}/k_{ib} + 1} \quad (2b)$$

$$\% B = \frac{1}{k_{br}/k_{rb} + k_{bi}/k_{ib} + 1} \quad (2c)$$

These equations depend only on the ratios k_{br}/k_{rb} and k_{bi}/k_{ib}. As an example, for the dual beam case

$$\frac{k_{br}}{k_{rb}} = \frac{\gamma_{br}[I_1\epsilon_b(\nu_1) + I_2\epsilon_b(\nu_2)]}{\gamma_{rb}[I_1\epsilon_r(\nu_1) + I_2\epsilon_r(\nu_2)]} \quad (3)$$

and an analogous equation with i in place of r for k_{bi}/k_{ib}. The ϵ ratios can be determined from absorption spectra reported previously. Compositional determinations under various illumination frequencies have been reported in the literature for *Loligo pealii*. Using these data, best values for the γ (quantum efficiency) ratios can be determined. The ratios were found to be $\gamma_{br}/\gamma_{rb} \cong 0.65$ and $\gamma_{bi}/\gamma_{ib} \cong 1.70$.

The fractional concentrations we calculated were plotted for many frequencies and the resultant curves were adjusted for continuity and self-consistency ($R + B + I = 1.0$). These results are shown in Figure 2. The fractional concentrations in Figure 2 apply to only the case of one beam; the results for two beams can be calculated by inserting eq 3 in eq 2. However, if $I_1 \gg I_2$, a linear approximation can be used with only small errors, giving

$$\% x \text{ with 2 beams} = \frac{I_1}{I_1 + I_2}(\% x \text{ at } \nu_1) + \frac{I_2}{I_1 + I_2}(\% x \text{ at } \nu_2) \quad (4)$$

References

Applebury, M. L., Zuckerman, O. M., Lamola, A. A., & Jovin, T. M. (1974) *Biochemistry 13,* 3448.

Aton, B., Doukas, A. G., Callender, R. H., Becher, B., & Ebrey, T. G. (1977) *Biochemistry 16,* 2995.

Azuma, K., Azuma, M., & Suzuki, T. (1975) *Biochim. Biophys. Acta 393,* 510.

Burke, M. J., Pratt, D. C., Faulkner, J. R., & Moscowitz, A. (1973) *Exp. Eye Res. 17,* 557.

Busch, G. E., Applebury, M. L., Lamola, A., & Rentzepis, P. M. (1972) *Proc. Natl. Acad. Sci. U.S.A. 69,* 2802.

Callender, R., & Honig, B. (1977) *Annu. Rev. Biophys. Bioeng. 6,* 33.

Callender, R., Doukas, A., Crouch, R., & Nakanishi, K. (1976) *Biochemistry 15,* 1621.

Chan, W. K., Nakanishi, K., Ebrey, T. G., & Honig, B. (1974) *J. Am. Chem. Soc. 96,* 3642.

Collins, D., Cookingham, R., & Lewis, A. (1977) *Appl. Opt. 16,* 252.

Cookingham, R., & Lewis, A. (1978) *J. Mol. Biol. 119,* 569.

Cookingham, R., Lewis, A., Collins, D., & Marcus, M. (1976) *J. Am. Chem. Soc. 98,* 2759.

Cookingham, R., Lewis, A., & Lemley, A. (1978) *Biochemistry 17* (preceding paper in this issue).

Ebina, Y., Nagasawa, N., & Tsukahara, Y. (1975) *Jpn. J. Physiol. 25,* 217.

Ebrey, T., Govindjee, R., Honig, B., Pollack, E., Chan, W., Crouch, R., Yudd, A., & Nakanishi, K. (1975) *Biochemistry 14,* 3933.

Gill, D., Heyde, M. E., & Rimai, L. (1971) *J. Am. Chem. Soc. 93,* 6228.

Goldschmidt, C., Ottolenghi, M., & Rosenfeld, R. (1976) *Nature (London) 263,* 169.

Green, B. H., Monger, T. G., Alfano, R. R., Aton, B., & Callender, R. H. (1977) *Nature (London) 269,* 179.

Heyde, M. E., Gill, D., Kilponen, R. G., & Rimai, L. (1971) *J. Am. Chem. Soc. 93,* 6776.

Honig, B., & Ebrey, T. (1974) *Annu. Rev. Biophys. Bioeng. 3,* 151.

Honig, B., Greenberg, A. D., Dinur, D., & Ebrey, T. G. (1976) *Biochemistry 15,* 4593.

Hubbard, R., & St. George, R. (1958) *J. Gen. Physiol. 41,* 501.

Kropf, A., Whittenberger, B. P., Goff, P., & Waggoner, A. S. (1973) *Exp. Eye Res. 17,* 591.

Lewis, A. (1978) *Proc. Natl. Acad. Sci. U.S.A. 75,* 549.

Lewis, A., & Spoonhower, J. (1974) *in Neutron, X-Ray and Laser Spectroscopy in Biophysics and Chemistry* (Yip, S., & Chen, S., Eds.) pp 347–376, Academic Press, New York, N.Y.

Lewis, A., Fager, R., & Abrahamson, E. (1973) *J. Raman Spectrosc. 1,* 465.

Lewis, A., Spoonhower, J., Bogomolni, R., Lozier, R., & Stoeckenius, W. (1974) *Proc. Natl. Acad. Sci. U.S.A. 71,* 4462.

Lewis, A., Spoonhower, J., & Perreault, G. J. (1976) *Nature (London) 260,* 675.

Marcus, M. A., & Lewis, A. (1977) *Science 195,* 1328.

Marcus, M. A., & Lewis, A. (1978a) *Biochemistry, 17* (following paper in this issue).

Marcus, M. A., & Lewis, A. (1978b) *Photochem. Photobiol.* (in press).

Marcus, M. A., Lewis, A., Racker, E., & Crespi, H. (1977) *Biochem. Biophys. Res. Commun. 78,* 669.

Mathies, R., & Stryer, L. (1976) *Proc. Natl. Acad. Sci. U.S.A. 73,* 2159.

Mathies, R., Oseroff, A., & Stryer, L. (1976) *Proc. Natl. Acad. Sci. U.S.A. 73,* 1.

Mathies, R., Friedman, T. B., & Stryer, L. (1977) *J. Mol. Biol. 109,* 367.

Oseroff, A. R., & Callender, R. H. (1974) *Biochemistry 13,* 4243.

Pepperberg, D. R., Lurie, M., Brown, P. K., & Dowling, J. E. (1976) *Science 191,* 394.

Perreault, G., Cookingham, R., Spoonhower, J., & Lewis, A. (1976) *Appl. Spectrosc. 30,* 614.

Peters, K., Applebury, M. L., & Rentzepis, P. M. (1977) *Proc. Natl. Acad. Sci. U.S.A. 74,* 3119.

Placzek, G. (1934) *Rayleigh and Raman Scattering,* UCRL translation 526L, Chapter 8.

Rimai, L., Gill, D., & Parsons, J. L. (1971) *J. Am. Chem. Soc. 93,* 1353.

Rimai, L., Heyde, M. E., & Gill, D. (1973) *J. Am. Chem. Soc. 95,* 4493.

Rosenfeld, T., Honig, B., Ottolenghi, M., Hurley, J., & Ebrey, T. G. (1977) *Pure Appl. Chem. 49,* 341.

Sperling, L., & Hubbard, R. (1975) *J. Gen. Physiol. 65,* 235.

Sulkes, M., Lewis, A., Lemley, A., & Cookingham, R. (1976) *Proc. Natl. Acad. Sci. U.S.A. 73*, 4266.

Suzuki, H., & Mizuhashi, S. (1964) *J. Phys. Soc. Jpn. 19*, 724.

Suzuki, T., Uji, K., & Kito, Y. (1976) *Biochim. Biophys. Acta 428*, 321.

Tang, J., & Albrecht, A. C. (1970) in *Raman Spectroscopy*, (Szymanski, H., Ed.) Vol. 2, pp 33-67, Plenum Press, New York, N.Y.

Tokunoga, T., Schichida, Y., & Yoshizawa, T. (1975) *FEBS Lett. 55*, 229.

Tokunaga, F., Govindjee, R., Ebrey, T. G., & Crouch, R. (1977) *Biophys. J. 19*, 191.

Warshel, A. (1977) *Annu. Rev. Biophys. Bioeng. 6*, 273.

Warshel, A., & Karplus, M. (1974) *Calculation of the Resonance Raman Intensities of Schiff Bases of Retinal*, preprint.

Yoshizawa, T., & Wald, G. (1963) *Nature (London) 197*, 1279.

Yoshizawa, T., & Wald, G. (1964) *Nature (London) 201*, 340.

Resonance Raman Spectroscopy of the Retinylidene Chromophore in Bacteriorhodopsin (bR_{570}), bR_{560}, M_{412}, and Other Intermediates: Structural Conclusions Based on Kinetics, Analogues, Models, and Isotopically Labeled Membranes†

Michael A. Marcus‡ and Aaron Lewis*

ABSTRACT: Resonance Raman spectra of various intermediates in the bacteriorhodopsin proton pumping cycle have been obtained at physiological and low temperatures. To interpret these data, spectra of model compounds, bacteriorhodopsin analogues, and isotopically labeled membranes have been measured. These results demonstrate that a protein group interacts with the Schiff base proton and, thus, the chromophore in protonated bacteriorhodopsin species is not a simple protonated Schiff base. This accounts for the abnormally low frequency of the $C{=}N^+H$ vibrational mode in bacteriorhodopsin and other failures to model the chromophore in bR_{570} with a simple butylamine protonated Schiff base of *all-trans*-retinal. To obtain the resonance Raman spectrum of M_{412} at physiological pH and temperatures, a dual beam kinetic technique was developed. We demonstrate that in the fingerprint region of the resonance Raman spectrum M_{412} is modeled accurately by a simple unprotonated butylamine Schiff base of *all-trans*-retinal. Spectral resolution and the solution environment of the membrane suspensions play important roles in this conclusion. Kinetic resonance Raman techniques are also used to monitor the time evolution of the M_{412} species and the intermediates which precede it. We find spectral features in our kinetic data which can be assigned to L_{550}, and we present evidence for a new unprotonated species (X) which occurs before M_{412}. Single pass flow resonance Raman spectra of bR_{560} also have been obtained, and, although bR_{570} and M_{412} appear to have all-trans chromophores, there are 13-cis-like features in the spectra of bR_{560}, L_{550}, and X.

Bacteriorhodopsin, the recently discovered pigment in the purple membrane of *Halobacteri n halobium* (Oesterhelt & Stoeckenius, 1971), has already d a significant impact on the fields of bioenergetics, act transport through membranes, and visual excitation. It nas been demonstrated that this rhodopsin-like pigment acts as a light-driven proton pump (Oesterhelt & Stoeckenius, 1973; Racker & Stoeckenius, 1974; Danon & Stoeckenius, 1974), and one of the functions of the H^+ gradient generated is to act as a driving force for ATP synthesis (Danon & Stoeckenius, 1974; Racker & Stoeckenius, 1974) in agreement with the Mitchell hypothesis (Mitchell, 1961, 1966). Thus, the molecular mechanism of active transport in this energy transducer is of considerable interest.

Resonance Raman spectroscopy is a technique which is capable of yielding important molecular information on the proton pumping function of this membrane-bound protein since it is environmentally and structurally sensitive to the conformation of chromophores in proteins (Lewis & Spoonhower, 1974). In fact, the application of this technique to bacteriorhodopsin has already yielded important structural (Mendelsohn, 1973, 1976; Lewis et al., 1974; Mendelsohn et al., 1974; Aton et al., 1977) and dynamic (Marcus & Lewis, 1977; Campion et al., 1977) information on this protein's active site.

In an early investigation (Lewis et al., 1974), we realized that bacteriorhodopsin, like rhodopsins in visual photoreceptors, undergoes light-induced conformational transformations which are thermally driven subsequent to the photochemical event. Therefore, low temperature techniques were utilized in this study (Lewis et al., 1974) to control the conformational states (intermediates) of the system. From these experiments we were able to show that, although bacteriorhodopsin (bR_{570}) is protonated and can be deuterated, M_{412}, the intermediate preceding the formation of the proton gradient, is unprotonated. The above data suggested that light absorption by the chromophore induces proton movements which are an essential part of this rhodopsin-like system. Furthermore, this investigation indicated that the chromophore was involved not only

† From the School of Applied and Engineering Physics, Cornell University, Ithaca, New York 14853. *Received February 22, 1978; revised manuscript received June 28, 1978.* This work was supported by National Institutes of Health Grant No. EY01377 and starter grants from the Research Corporation and the Petroleum Research Fund, administered by the American Chemical Society. N.A.M. was a National Institutes of Health predoctoral fellow. A.L. was an Alfred P. Sloan Fellow.

‡ Present address: Kodak Research Laboratories, Physics Division, B-81, Kodak Park, Rochester, New York 14650.

0006-2960/78/0417-4722$01.00/0